A novel cross-linked polyzwitterion/anion having pH-responsive carboxylate and sulfonate groups for the removal of Sr 2+ from aqueous solution at low concentrations

1 AUTHOR:

Shamsuddeen A Haladu

University of Dammam

15 PUBLICATIONS **29** CITATIONS

A novel cross-linked polyzwitterion/anion having pH-responsive carboxylate and sulfonate groups for the removal of Sr^{2+} from aqueous solution at low concentrations

Shaikh A. Ali *, Shamsuddeen A. Haladu

Chemistry Department, King Fahd University of Petroleum & Minerals, Dhahran 31261, Saudi Arabia

ARTICLE INFO

ABSTRACT

A novel cross-linked polyzwitterion (CPZ) was synthesized *via* cycloterpolymerization of *N,N-diallyl-N-sulfopropylammonioethanoic acid* (92.5 mol%), a cross-linker 1,1,4,4-tetraallylpiperazinium dichloride (7.5 mol%), and sulfur dioxide (100 mol%) in the presence of azoisobutyronitrile in dimethylsulfoxide at 60 °C. CPZ, upon treatment with NaOH, was converted into a cross-linked polyzwitterion/anion (CPZA). The experimental data for the adsorption of Sr^{2+} on CPZA fitted the pseudo-second-order kinetic model and Freundlich as well as Temkin isotherm models. The adsorption process was spontaneous and exothermic in nature with negative values for both ΔG and ΔH. The low activation energy of 7.18 kJ/mol indicated the adsorption as a favorable process. The removal for the initial concentrations of 200 ppb and 1000 ppb (i.e., 1 ppm) of Sr^{2+} ions was observed to be 87% and 92%, respectively. An efficient synthetic access to the resin and excellent adsorption capacity and desorption would enable its use in the treatment of radioactive nuclear waste containing Sr^{2+} ions. The CPZA provided an opportunity to test the efficacy of a zwiiterionic/anionic group in the removal of Sr^{2+} ions in low concentrations.

© 2013 Elsevier Ltd. All rights reserved.

1. Introduction

Radioactive wastes containing a variety of radionuclides severely pollute the environment. Fission product like ^{89}Sr and ^{90}Sr with half-lives of 51 days and 29 years, respectively [1], can contaminate underlying layers of soil and groundwater [2,3]. Strontium's resemblance to calcium enables its easy incorporation into bone and by virtue of being a very strong β-emitter, it leads to the development of bone sarcoma and leukemia [1,4,5]. It is thus quite necessary to remove Sr, one of the most hazardous elements, from wastewater. Adsorption with solid adsorbents like polyacrylonitrile/zeolite composite [6], bentonite [7], zeolites and clays have been studied for the removal of Sr^{2+} ions [8,9], and the adsorption capacity is found to be somewhat low. Derivatives of crown ethers [10,11], cross-linked polymers containing carboxyl motifs [12,13] including gels based on carboxylated polysaccharide derivatives [14] were also used to adsorb Sr^{2+} ions.

A study of 2Na$^+$ → Sr^{2+} exchange equilibria with actual ground water using a synthetic clay revealed high capacity for uptake of ^{90}Sr [15]. A study of adsorption of Sr^{2+} from sulfuric acid solution by different Dowex 50W-X ion exchange resins has been investigated [16]. Among these resins, Dowex 50W-X8 resin

showed the maximum sorption of Sr^{2+} from the aqueous solutions. Inorganic cation exchange materials such as niobate molecular sieves [17], titanate [18], and synthetic micas [19] have been studied for the removal of radioactive ions. A few separation processes of Sr^{2+} by liquid–liquid solvent extraction have also been reported [20–22].

Polyzwitterions synthesized from *N*-vinyl imidazole have been used as sorbents for the removal of Sr^{2+}. The polysulfobetaines (polyzwitterions) carrying both charges on the same repeating unit are good candidate for the water technologies on accounts of its dual role in removing the cationic or anionic effluent and they also can impart anti-microbial properties [23]. pH-responsive polyzwitterions are of great academic and industrial interest [24–27] and useful in water treatment, drag reduction, petroleum recovery, viscosification, coatings, and cosmetics [28]. Recently, the researchers have focused on the syntheses of zwitterionic cross-linked inorganic/organic hybrid materials for the removal of toxic heavy metal ions *via* electrostatic effects [29–31].

The literature presented above describes many sorbent materials to remove larger concentration of Sr^{2+} ions; however, it remains challenging to develop new materials for removing Sr^{2+} ions at ppb-levels. For the removal of metal ions, the materials developed so far include zwitterionic (±) or anionic (−) groups in which the anionic centers are the sites where the metal ions are physically or chemically attached. In the current study, a novel cross-linked polymer containing zwitterionic (±) and anionic (−) groups

* Corresponding author. Fax: +966 3 860 4277.
 E-mail address: shaikh@kfupm.edu.sa (S.A. Ali).
 URL: http://faculty.kfupm.edu.sa/CHEM/shaikh/ (S.A. Ali).

embedded in the same repeating unit has been synthesized and tested for efficiency as adsorbent for the removal of Sr^{2+} ions at low concentrations from aqueous solutions. To our knowledge, neither the synthesis of cross-linked polymer having zwitterionic/anionic group nor its use has been reported before; as such the study would establish the efficiency of this special functionality for the removal of metal ions.

2. Experimental

2.1. Physical methods

Elemental analysis was carried out on a Perkin–Elmer Elemental Analyzer Series II Model 2400. IR spectra were recorded on a Perkin–Elmer 16F PC FTIR spectrometer. ^1H and ^{13}C spectra were measured on a JEOL LA 500 MHz spectrometer using HOD signal at $\delta 4.65$ and dioxane signal at 67.4 ppm as internal standards, respectively. Atomic absorption spectroscopy (AAS) analysis was performed using AAS model iCE 3000 series (Thermo Scientific). The instrumental lower detection limit for Sr^{2+} ions was determined to be 15 ± 3 ppb. Scanning electron microscopy (SEM) images were taken by TESCAN LYRA 3 (Czech Republic) equipped with Oxford, energy-dispersive X-ray spectroscopy (EDX) detector model X-Max. Thermogravimetric analysis (TGA) was performed using a thermal analyzer (STA 429) manufactured by Netzsch (Germany). The polymer sample to be tested (usually ~5 mg) was placed in a platinum crucible. Aluminum oxide (Al_2O_3; ~4 mg) was placed in an identical platinum crucible as a reference sample. With the sample carrier system, which had two sets of 10% Pt–Pt/Rh thermocouples, the sample carrier was placed in the middle of the vertical furnace, which was programmed and controlled by a microprocessor temperature controller. The temperature was raised at a uniform rate of 10 °C/min. The analyses were made over a temperature range of 20–800 °C in an air atmosphere flowing at a rate of 100 mL/min.

2.2. Materials

Azoisobutyronitrile (AIBN) from Fluka AG was purified by crystallization from a chloroform–ethanol mixture. Diallylamine, from Fluka Chemie AG (Buchs, Switzerland) were used as received. Dimethylsulfoxide (DMSO) was dried over calcium hydride overnight and then distilled under reduced pressure at a boiling point of 64–65 °C (4 mm Hg). All solvents used were of analytical grade. Considering the high toxicity of radioactive ions, aqueous solutions of non-radioactive Sr^{2+} ions were used in sorption experiments. For this purpose, $Sr(NO_3)_2$ was purchased from Fisher Scientific Company (New Jersey, USA).

2.3. Synthesis of zwitterionic ester (**1**)

Zwitterionic monomer N-carboethoxymethyl-3-(N,N-diallylamino)propanesulfonate (**1**) was prepared in 82% yield by reacting an equimolar mixture of N,N-diallyl-N-carboethoxymethylamine [32] and 1,3-propanesultone in acetonitrile (130 cm^3 for 0.13 mol amine) at 72 °C for 72 h, mp (methanol/acetone/diethyl ether) 162–163 °C [33].

2.4. Acid hydrolysis of zwitterionic ester **1** to zwitterionic acid **2**

A solution of zwitterionic ester **1** (16.4 g, 53.7 mmol) in 6 M HCl (60 mL) was heated in a closed vessel at 80 °C for 27 h. The resulting solution was then freeze-dried to obtain **2** as a thick liquid which was crystallized from a mixture of MeOH/CH$_3$CN/diethylether as white crystals (14.2 g, 95%). (Found: C, 47.4; H, 7.0; N,

4.9; S, 11.3%. C$_{11}$H$_{19}$NO$_5$S requires C, 47.64; H, 6.91; N, 5.05; S, 11.56%); ν_{max} (KBr) 3500–2600 (br), 3015, 2980, 2930, 1728, 1642, 1479, 1400, 1324, 1197, 1166, 1081, 1040, 999, 972, 957, 941, 888, 801, 732, 698, 619, 596, 573, and 521 cm^{-1}; δ_H (D$_2$O) 2.07 (2H, quint, J 7.05 Hz), 2.77 (2H, t, J 6.7 Hz), 3.47 (2H, apparent t, J 7.95 Hz), 3.98–4.02 (6H, m), 5.56 (4H, m), 5.84 (2H, m), (HOD: 4.65); δ_C (D$_2$O) 18.36, 47.86, 56.82, 58.32, 62.68 (2C), 124.25 (2C), 130.42 (2C), 167.61 (dioxane: 67.40 ppm).

2.5. 1,1,4,4-Tetraallylpiperazinium dichloride (**3**)

Monomer **3**, a cross-linker, was prepared as described [34].

2.6. Terpolymerization of monomers **2**, **3** and sulfur dioxide to form cross-linked polyzwitterion (CPZ) **4**

Sulfur dioxide (1.28 g, 20 mmol) was absorbed in a mixture of **2** (5.55 g, 20 mmol) and cross-linker **3** (1.62 mmol, 0.52 g) in DMSO (7.0 g). Initiator AIBN (140 mg) was then added, and the mixture stirred at 65 °C for 24 h. At the end of the elapsed time, the hardened solid mass was soaked in water for 24 h, with frequent changing of water, and finally dried under vacuum at 55 °C to a constant weight (5.00 g, 68%). (Found: C, 39.2; H, 5.9; N, 4.2; S, 17.7%. monomer **2**/SO$_2$ C$_{11}$H$_{19}$NO$_7$S$_2$ (92.5 mol%) and monomer **3**/SO$_2$ C$_{16}$H$_{28}$Cl$_2$N$_2$O$_2$S (7.5 mol%) requires C, 39.56; H, 5.74; N, 4.34; S, 18.00%).

2.7. Basification of CPZ **4** to cross-linked polyzwitterion/anion (CPZA) **5**

A mixture of CPZ **4** (4.6 g, 13.4 mmol) and sodium hydroxide (0.74 g, 18.5 mmol) in water (150 ml) was stirred for 24 h, after which it was poured into excess methanol. The resin **5** was filtered and dried under vacuum at 55 °C to a constant weight (4.7 g, 97%) TGA analysis show initial decomposition around 250 °C). (Found: C, 37.5; H, 5.4; N, 4.1; S, 16.7%. monomer **2**/SO$_2$ C$_{11}$H$_{18}$NNaO$_7$S$_2$ (92.5 mol%) and monomer **3** (dihydroxide)/SO$_2$ C$_{16}$H$_{30}$N$_2$O$_4$S (7.5 mol%) requires C, 37.79; H, 5.27; N, 4.17; S, 17.02%).

2.8. Adsorption experiments

The procedure for the adsorption experiments of the cross-linked polymer CPZA **5** for Sr^{2+} ions can be described briefly as follows: a mixture of CPZA (50 mg) in an aqueous $Sr(NO_3)_2$ (1 mg L^{-1}) solution (20 mL) was stirred using a magnetic stir-bar at different pH for 24 h. The filtrate was analyzed by atomic absorption spectroscopy to determine the amount of Sr^{2+} remained. The adsorption capacity ($q_{Sr^{2+}}$) in mg g^{-1} can be calculated using the following equation:

$$q_{Sr^{2+}} = \frac{(C_0 - C_f)V}{W} \qquad (1)$$

where C_0 and C_f are the initial and final concentration of Sr^{2+} ions in mg L^{-1}, respectively, W is the weight of the polymer in g, and V is the volume of the solution in L. Data presented are average of triplicate runs and varied by less than 4% in all the cases studied. The values of adsorption capacity (q) at various times and equilibrium are denoted as q_t and q_e, respectively, whereas C_e is used to refer to the equilibrium metal concentration in the solution.

For adsorption kinetic studies, the resin sample was stirred in a 1 mg L^{-1} $Sr(NO_3)_2$ solution for different adsorption times at pH 3 at 296, 308 and 323 K. Based on the adsorption data from experiments carried out at different temperatures (296, 308 and 323 K), the pseudo-second-order rate constant (k_2) at various temperatures and the activation energy (E_a) for the adsorption process were determined (Section 3.5.2). Thermodynamic parameters ΔG, ΔH and ΔS for Sr^{2+} removal were calculated using q_e and C_e values for the adsorption experiments carried out as described above

using 1 mg L^{-1} Sr(NO$_3$)$_2$ solution. The adsorption isotherms were constructed by changing the concentration of Sr(NO$_3$)$_2$ solution from 200 μg L^{-1} (i.e. ppb) to 1000 μg L^{-1} at 296 K for 24 h.

2.9. Desorption experiment

Adsorption of Sr^{2+} ions was performed by stirring 50 mg resin in aqueous Sr(NO$_3$)$_2$ (1 mg L^{-1}) solution (20 mL) for 24 h. The amount of Sr^{2+}adsorbed (i.e., q$_{Sr}$2+) was determined as described in the above section. The loaded resin was then filtered, dried and quantitatively transferred to a stirring 0.1 M HNO$_3$ (20 mL) for 24 h for the desorption experiment. After filtration, the amount of Sr^{2+} ions desorbed in the filtrate (∼19 mL) was determined; the efficiency of the desorption process was calculated by the ratio of desorbed amount of Sr^{2+} ions to the amount of adsorbed Sr^{2+} ions (i.e., q$_{Sr}$2+) in the resin.

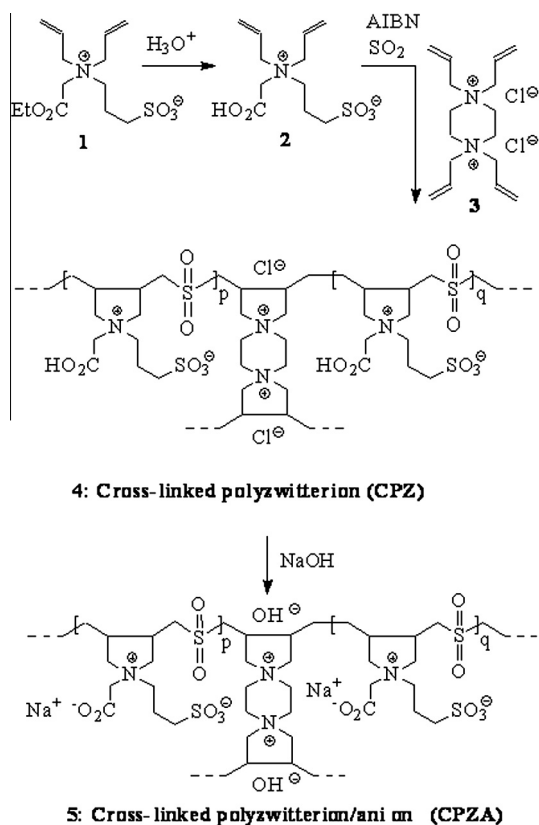### 2.10. FTIR spectroscopy

Unloaded and loaded resins were investigated by FTIR spectroscopy. Unloaded resins (30 mg) were immersed in 0.1 M Sr(NO$_3$)$_2$ solution (10 mL) for 4 h at a pH of 3, filtered, and dried under vacuum until constant weight was achieved.

3. Results and discussion

3.1. Synthesis of cross-linked polyzwitterion/anion (CPZA **5**)

Butler's cyclopolymerization protocol has been utilized to synthesize the current resin **5** (Scheme 1). Butler's pioneering discovery of the cyclopolymerization involving a variety of *N,N*-diallylammonium monomers has led to the synthesis of an array of scientifically and technologically important water-soluble cationic polyelectro-
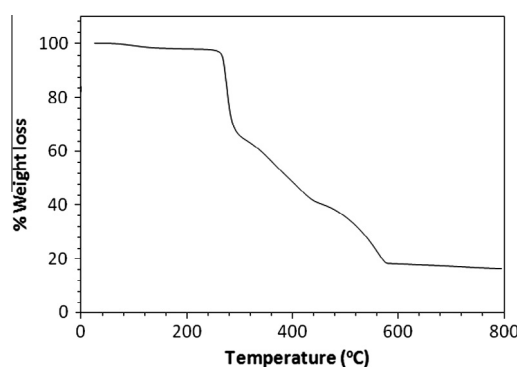

Fig. 1. TGA curve of CPZA **5**.

lytes [35–37]. The polymer-architecture, having the five-membered cyclic units embedded in the backbone, has been recognized as the eighth major structural type of synthetic polymers [36]. Over 33 million pounds of poly(diallyldimethylammonium chloride) alone are sold annually for water treatment and another 2 million pounds are used for personal care formulation [37]. Recently, a pH-responsive cross-linked polyzwitterion containing phosphonate motifs has been synthesized *via* Butler's cyclopolymerization and tested for the removal of heavy metal ions [38].

Zwitterionic ester **1** [33], prepared by reacting an equimolar mixture of *N,N*-diallyl-*N*-carboethoxymethylamine and 1,3-propanesultone in acetonitrile on acidic hydrolysis afforded the zwitteionic acid **2** in excellent yield (95%) (Scheme 1). Ester hydrolysis was ascertained by NMR spectroscopy and elemental analysis (Experimental). Thus the conversion of the ester moiety CO$_2$CH$_2$CH$_3$ in **1** to CO$_2$H in **2** was confirmed by the absence of ethyl protons and carbons in the NMR spectra of the later. The CH$_3$ proton and CH$_3$ carbon of the CO$_2$CH$_2$CH$_3$ group in **1** were reported to appear at δ1.28 and 64.46 ppm, respectively [33].

A mixture of monomer **2** (92.5 mol%), cross-linker **3** (7.5 mol%), and SO$_2$ (100 mol%) in solvent DMSO underwent cyclocopolymerization in the presence of initiator AIBN to give cross-linked polyzwitterion (CPZ **4**) (Scheme 1) as a white solid. CPZ **4** upon treatment with excess NaOH led to the formation of cross-linked polyzwitterion/anion CPZA **5**. To the best of our knowledge this is the first cross-linked polymer *via* Butler's cyclopolymerization protocol that
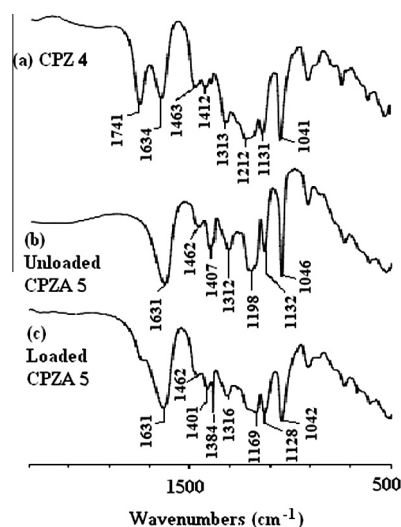

Scheme 1. Synthesis cross-linked polyzwitterion/anion polymers.

Fig. 2. IR spectra of (a) cross-linked CPZ **4**; (b) CPZA **5**; and (c) CPZA **5** loaded with Sr^{2+}.
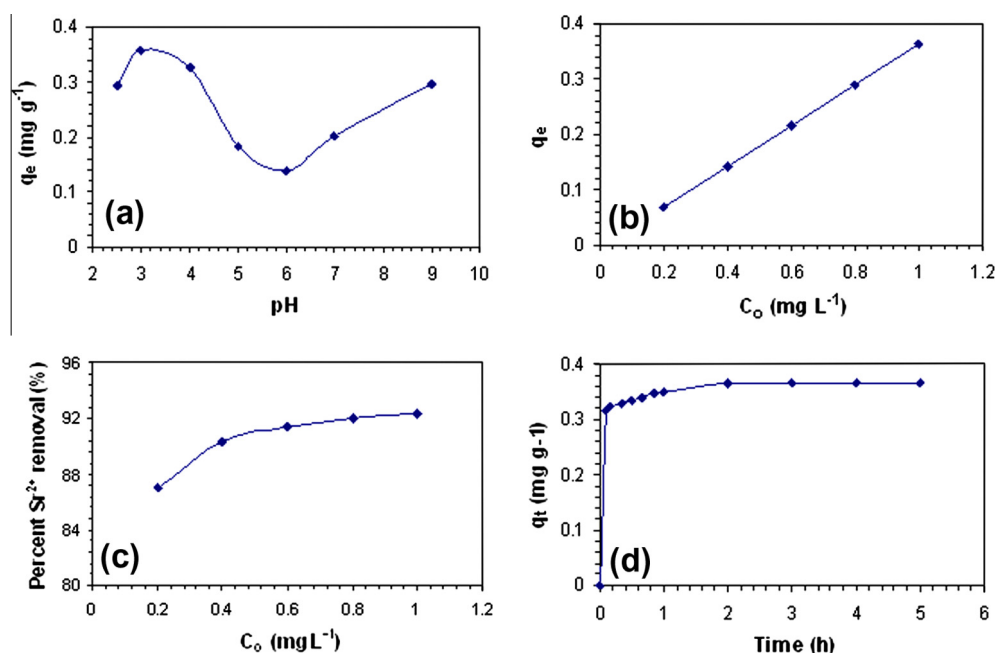
Fig. 3. (a) The effect of pH on the adsorption capacity of CPZA **5** at Sr^{2+} initial concentration of 1.00 ppm for 24 h at 23 °C; (b) The effect of initial concentration of Sr^{2+} on the adsorption capacity of CPZA **5** at pH 3 for 24 h at 23 °C; (c) The percent removal of Sr^{2+} at its various initial concentrations at pH 3 for 24 h at 23 °C; and (d) Absorption kinetic curve of Sr^{2+} in 1.00 ppm Sr^{2+} solution at pH 3 at 23 °C.
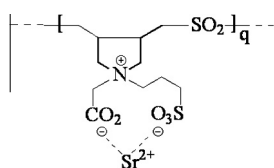
Scheme 2. Adsorption of Sr^{2+} on CPZA **5**.

ensured the embedding of the zwitterionic as well as anionic groups in each repeating unit. Elemental analysis of CPZ **4** and CPZA **5** confirmed the incorporation of monomer **2** and cross-linker **3** into the polymer in an approximate mol ratio of 93:7, which is similar to the feed ratio.

Thermogravimetric analysis (TGA) curve of CPZA **5** (Fig. 1) showed two major loss in weight: first slow weight loss of 4.0% is attributed to loss of water imbedded inside the cross-linked polymer, the second major loss of 28% around 250 °C is attributed to the loss SO_2, and the third major loss of 52% is the result of combustion of nitrogenated organic fraction with the release of CO_2, NO_x and H_2O gases [39]. The residual mass at 800 °C was found to be 16%.

3.2. FTIR characterization of monomers and polymers

The IR spectrum of zwitterionic monomer **2** indicates the presence of sulfonate group by its strong characteristic bands at 1197 $cm^{-1}$and 1040 cm^{-1} [40], while the absorption at 1728 cm^{-1} is attributed to C=O stretch of COOH [41]. The corresponding adsorptions for the CPZ **4** appear at 1212, 1041, and 1741, respectively (Fig. 2a). The symmetric and antisymmetric stretching of COO⁻ in the dipolar form [41] of CPZ **4** were observed at 1412 and 1634 cm^{-1}, respectively (Fig. 2a). The two moderately strong bands at 1313 cm^{-1} and 1131 cm^{-1} were assigned to the asymmetric and symmetric vibrations of SO_2 unit [39] (Fig. 2a).

For the unloaded resin CPZA **5**, the absorption due to C=O stretch of COOH was missing, instead the symmetric and antisymmetric

stretching of COO⁻ appeared at 1407 and 1631 cm^{-1} (Fig. 2b). The appearance of a new band at 1384 cm^{-1} (Fig. 2c) was attributed to the presence of ionic nitrate group since the adsorption process was carried out in the presence of $Sr(NO_3)_2$ [42]. Interestingly, the presence of this band implies the ability of the resin to act also as an anion exchanger. Note that the absorption band attributed to the nitrate ion is absent in the IR spectrum of the unloaded resin **5** (Fig. 2b). The IR spectra of the resin loaded with Sr^{2+} (Fig. 2c) revealed the increase in the intensity and broadness of the C=O vibrations as a result of the adsorption of the metal ions [43].

3.3. Effect of pH and temperature on adsorption

The effect pH (in the range 2.5–9) on the uptake of Sr^{2+} was investigated at a fixed concentration (1 mg L^{-1}) and time of 24 h at 23 °C. The pH of the media was controlled by acetic acid/sodium acetate buffer in the lower pH range while ammonia/ammonium chloride buffer was used in the higher pH range. To attain a pH of 2.5, additional amount of HCl was added to the buffer solution. Results of metal uptake at different pH are shown in Fig. 3a. Optimum pH was found to be 3; after reaching the minimum at pH 6, the adsorption capacity increases on further increasing the pH. Sr^{2+} ions may be captured by carboxyl and sulfonate groups by chelation as depicted in Scheme 2. It is worth mentioning that pK_a of CO_2H and SO_3H groups in this resin are expected to +2.5 and −2.1, respectively [41]. At pH 3 or even at 2, a sizable proportion of CO_2^- will exist in the acid–base equilibrium and almost the entire SO_3H will remain in the dissociated form of SO_3^-.

The adsorption of Sr^{2+} reaches a maximum at a pH of 3. At pH values <3, the abundant H^+ ions in the solution will compete with Sr^{2+} ions to combine with CO_2^- or SO_3^- groups, while plentiful Cl^- ions will shield the positive nitrogens of the sulfobetaine zwitterionic groups. The decrease of adsorption with the increase of pH in the range 3–6 and reaching a minimum at pH 6 is somewhat baffling even though there are some literature precedences. Thus the adsorption of Sr^{2+} on a hybrid gel prepared from bis(trimethoxysilylpropyl)amine is reported to reach a maximum at a pH of

Table 1
Lagergren kinetic model parameters for Sr^{2+} adsorption.

Temp (K)	$q_{e,exp}$ (mg g^{-1})	k_2 (h^{-1} g mg^{-1})	h^a (h^{-1} g^{-1} mg)	$q_{e,cal}$ (mg g^{-1})	R^2	E_a (kJ mol^{-1})
Pseudo second-order						
296	0.365	72.2	9.80	0.369	0.9998	7.18
308	0.352	82.3	10.3	0.354	0.9991	
323	0.336	92.2	10.5	0.338	0.9995	

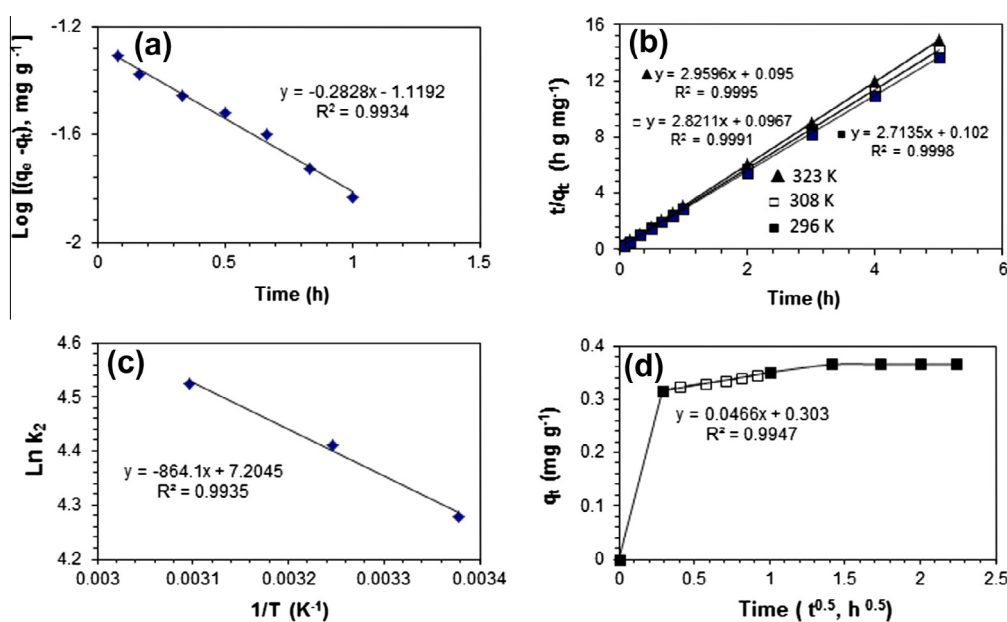| Temp (K)	$q_{e,exp}$ (mg g^{-1})		k_1 (h^{-1})		$q_{e,cal}$ (mg g^{-1})		R^2
Pseudo first-order							
296	0.365		0.651		0.0760		0.9934

[a] Initial adsorption rate $h = k_2 q_e^2$.

Fig. 4. (a) Lagergren first-order kinetic model for adsorption of Sr^{2+} (1.00 ppm) on CPZA **5** at pH 3 at 23 °C; (b) Pseudo-second-order kinetic model for adsorption of Sr^{2+} (1.00 ppm) on CPZA **5** at pH 3 at 23 °C; (c) Determination of the activation energy for Sr^{2+} adsorption on CPZA **5**; and (d) Intraparticle diffusion plot for of Sr^{2+} adsorption on CPZA **5** at pH 3 at 23 °C.

4.7, minimum at 7.3 and further increase at higher pH values [44]. A polyacrylonitrile/zeolite composite adsorbent has been shown to have maximum adsorption of Sr^{2+} at a pH of 5.2 and at higher pHs the percent adsorption capacity decreases [6]. The percent removal for Sr^{2+} by a zwitterionic polysulfobetaine has been shown to have a minimum at pH 5.8 [45]. It is to be noted that Sr^{2+} could form mono-valent ionic pairs such as $SrCl^+$ and $SrOH^+$ before being adsorbed [44,46]. Sr in the pH range 1–11 can be present in the form of Sr^{2+} and a very negligible $Sr(OH)^+$ which increases in concentration above 10 [6]. There are many factors that may affect the adsorption behavior. The pH of the media may affect the network characteristics such as pore size, the water uptake as well as the ion uptake behavior of the resin. The adsorption in the form mono-valent ion pair like $SrCl^+$ requires one exchange site while a divalent Sr^{2+} is expected to demand two exchange sites. Neither the reported articles nor our current work are able to provide an effective rationale for the observed minimum around pH 6.

The rest of the adsorption studies were carried out at the optimal pH of 3.

3.4. Effect of initial concentration on the adsorption of Sr^{2+} ions

As shown in Fig. 3b, the adsorption capacity of CPZA **5** increased with increasing concentrations of Sr^{2+} ions. The percent removal

for the initial concentrations of 200 ppb and 1000 ppb (i.e. 1 ppm) was determined to be 87 and 92, respectively (Fig. 3c).

3.5. Adsorption kinetics

The adsorption kinetics, which describes the relationship between adsorption capacity and adsorption time, is presented in Fig. 3d. The adsorption process was found to be fast and it reached the equilibrium within 2 h indicating the strong ability of this resin to remove Sr^{2+} ions from aqueous solutions.

3.5.1. Lagergren first-order and pseudo-second-order kinetics

Lagergren first-order kinetics describes the adsorption process in a solid–liquid system based on the adsorption capacity of the solid, where it assumes that one metal ion is adsorbed onto one adsorption site on the surface of the adsorbent [47]. The linear form of the model can be described in the following equation:

$$\log(q_e - q_t) = \log q_e - \frac{k_1 t}{2.303} \tag{2}$$

where q_e and q_t (mg g^{-1}) are the adsorption capacities at equilibrium and at time t (h), respectively, and k_1 is the first-order rate constant. The k_1 and q_e were evaluated experimentally using the slope and intercept of the plots of $\log(q_e - q_t)$ versus t (Table 1 and Fig. 4a). The fitness of the data was found to be excellent having
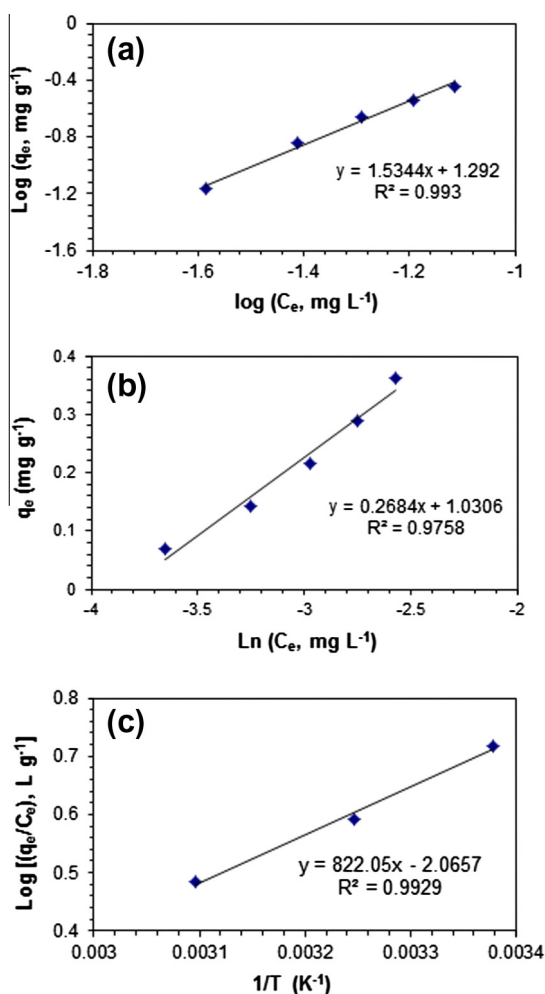
Fig. 5. (a) Freundlich isotherm for Sr^{2+} adsorption on CPZA **5**; (b) Temkin isotherm for Sr^{2+} adsorption on CPZA **5**; and (c) plot of $\log(q_e/C_e)$ versus $(1/T)$.

Table 2
Freundlich and Temkin isotherm model constants for Sr^{2+} adsorption.

Freundlich isotherm model		
k_f (mg$^{1-1/n}$ g^{-1} L$^{1/n}$)	n	R^2
19.6	0.652	0.9930
Temkin isotherm model		
A (L g^{-1})	B (J/mol)	R^2
46.5	0.268	0.9758

Table 3
Thermodynamic data for Sr^{2+} adsorption.

Temperature (K)	ΔG (kJ/mol)	ΔH (kJ/mol)	ΔS (J/mol K)	R^2
296	−4.03	−15.7	−39.5	0.9929
308	−3.56			
323	−2.97			

square of regression coefficient (R^2) of 0.9934; only the low time zone linear fit, not the longer time fit, was considered. However, agreement between experimentally observed equilibrium adsorption ($q_{e,exp}$ = 0.365 mg g^{-1}) and that derived using 1st order equation is very poor ($q_{e,cal}$ = 0.0760 mg g^{-1}) thereby indicating that the adsorption process does not fit with Lagergren first-order kinetic model (Table 1) [48].

The linear pseudo-second-order kinetic model [49] can be expressed by the following equation:

$$\frac{t}{q_t} = \frac{1}{k_2 q_e^2} + \frac{t}{q_e}$$

(3)

where k_2 is pseudo-second-order rate constant, q_t and q_e are the respective adsorption capacity of the metal ions at a time t and at equilibrium.

It is evident from Fig. 4b and Table 1 that the pseudo-second-order kinetic model fitted well with the adsorption of Sr^{2+} indicating that the adsorption process might be a chemical adsorption [50]. Also the equilibrium adsorption capacities ($q_{e,cal}$: 0.369 mg g^{-1}) derived from Eq. (3) are in close agreement with those observed experimentally ($q_{e,exp}$: 0.365 mg g^{-1}) at 23 °C. The experimental data so far revealed that the resin is an efficient adsorbent for the removal of Sr^{2+} ions from aqueous solutions.

3.5.2. Adsorption activation energy
The adsorption activation energy can be deduced from the rate constants (k_2) obtained form the pseudo-second-order kinetic model (Table 1) using the Arrhenius equation (Eq. (4)) expressed as:

$$\ln k_2 = -\frac{E_a}{2.303RT} + \text{constant}$$

(4)

where k_2 is the second order rate constant (g mg^{-1} h), E_a the activation energy (kJ mol^{-1}), R is the universal gas constant (8.314 J mol^{-1} K) and T is the solution temperature (K). A plot of $\ln k_2$ versus $1/T$ gives a linear plot, with slope $-E_a/R$ (Fig. 4c and Table 1). The low activation energy value of 7.18 kJ mol^{-1} is an indication of the feasibility of the adsorption process [48,51].

3.5.3. Intraparticle diffusion model
The mechanism of adsorption can be understood by determining the rate-limiting step, and this can be determined by using some adsorption diffusion models which are always constructed on the basis of three consecutive steps: (1) film diffusion (i.e., diffusion across the liquid film surrounding the adsorbent particles); (2) intraparticle diffusion (i.e., diffusion in the liquid contained in the pores and/or along the pore walls); and (3) mass action (i.e., fast physical adsorption and desorption between the adsorbate and active sites). The intraparticle diffusion model assumes that the metal ions are transported from the solution through an interface between the solution and the adsorbent (i.e., film diffusion) followed by a rate-limiting intraparticle diffusion step which bring them into the pores of the particles in the adsorbent. Following equation expresses the relation of the adsorption capacity and time [52–54]:

$$q_t = x_i + k_p t^{0.5}$$

(5)

where q_t is the adsorption capacity at time t, k_p is the rate constant of intraparticle diffusion, x_i is related to boundary layer thickness. According to the Weber–Morris model [47,49], a straight line fit for the plot of q_t versus $t^{0.5}$ passing through the origin implies the intraparticle diffusion as the rate-limiting step [55]. Since the initial linear plot did not pass through the origin, that is, there is an intercept which indicates that rapid adsorption occurs within a short period of time (Fig. 4d).

The intercept x_i of the linearized line was used to define the initial adsorption factor (R_i) as:

$$R_i = 1 - \frac{x_i}{q_e}$$

(6)

where x_i is the initial adsorption amount and q_e the final adsorption amount at the longer time. The x_i and q_e values of 0.303 and 0.365 mg g^{-1}, respectively, gave an R_i value of 0.17 which means
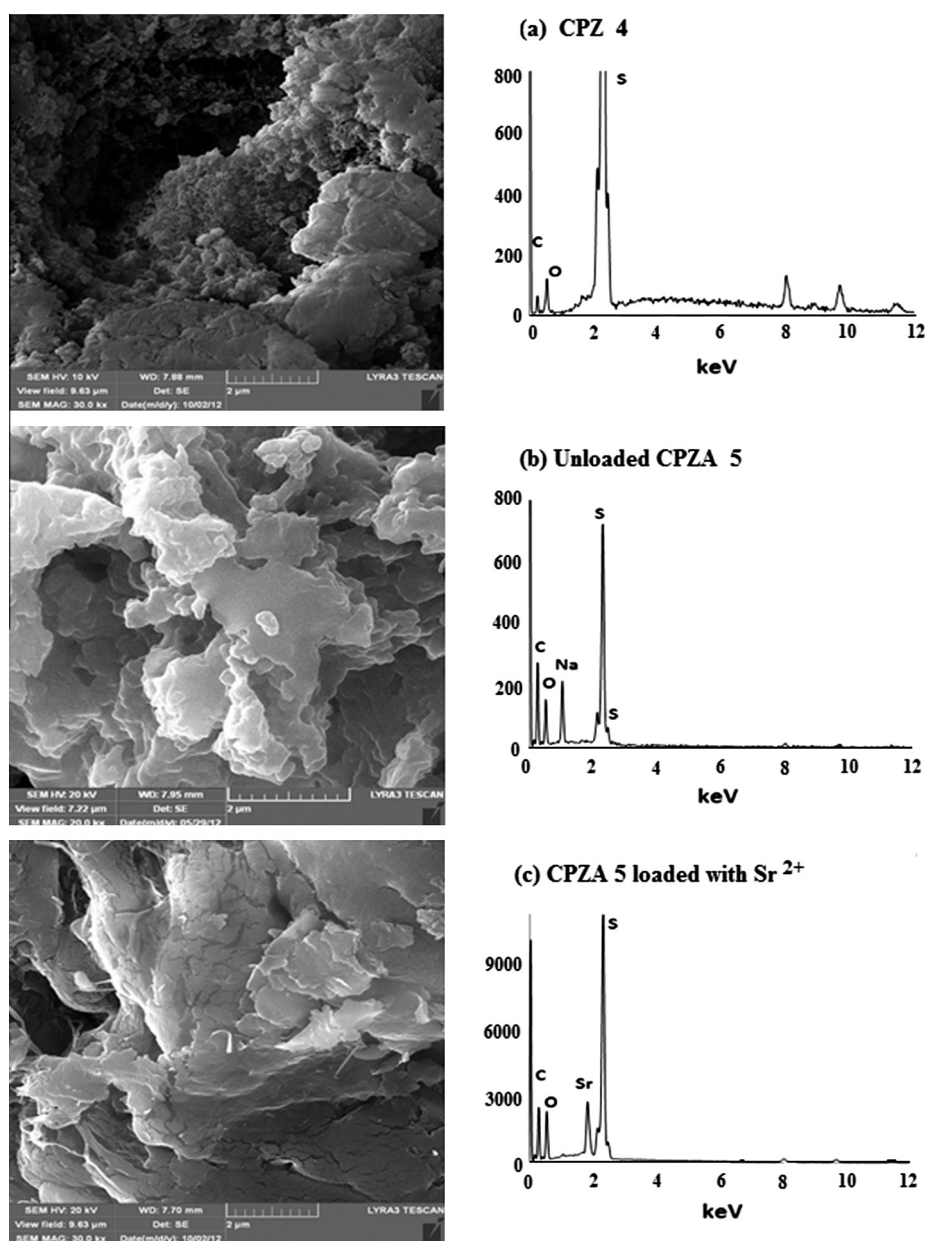
Fig. 6. SEM images for (a) unloaded CPZ **4** and (b) unloaded CPZA **5** and loaded **5** with Sr²⁺.

that the relatively strong rapid initial adsorption has already reached 83% before the first adsorption data was collected at a time of 5 min. The other 17% of adsorption is governed by intraparticle diffusion as indicated by the linear relation with an excellent square of correlation coefficient (R^2) of 0.9947 (Fig. 4d). In this case, the intraparticle diffusion within the pores of the resins was the rate-limiting step. Note that the last linear section represents the final equilibrium stage.

3.6. Adsorption isotherms

As shown in Fig. 3b, the adsorption capacity of CPZA **5** increases with the increase in the initial concentration of Sr²⁺ ions. To further explore the adsorption mechanism, Langmuir, Freundlich and Temkin isotherm models were used to analyze the adsorption data. The Langmuir isotherm model [56,57], which assumes the mechanism of the adsorption process as a monolayer adsorption on com-

pletely homogeneous surfaces where interactions between adsorbed molecules are negligible, can be expressed by the following equation:

$$\frac{C_e}{q_e} = \frac{C_e}{Q_m} + \frac{1}{Q_m b} \tag{7}$$

where C_e and q_e are the concentrations of metal ion in the solution and resin, respectively, Q_m and b are the Langmuir constants. The Langmuir plot of C_e/q_e versus C_e enables the calculation of Langmuir constants from the intercept and slope of the linear plot. The adsorption of Sr²⁺ by the resin did not fit the Langmuir isotherm model, so the relevant graph has not been displayed.

Freundlich isotherm model, which describes the non-ideal adsorption occurring on a heterogeneous surface with uniform energy as well as multilayer adsorption, are expressed by the following equations:

$$q_e = k_f C_e^{1/n} \tag{8}$$

$$\log q_e = \log k_f + \frac{1}{n} \log C_e \tag{9}$$

where k_f and n represent the Freundlich constants, which can be calculated from the slope and intercept of the linear plot of $\log q_e$ versus $\log C_e$ as presented in Fig. 5a. The value of n was determined to be 0.652. A $1/n$ value above unity implies cooperative adsorption [58].

The Temkin isotherm equation assumes that the heat of adsorption of all the molecules in layer decreases linearly with coverage due to adsorbent-adsorbate interactions, and that the adsorption is characterized by a uniform distribution of the bonding energies up to some maximum binding energy. The Temkin isotherm [59,60] has been used in the following form:

$$q_e = \frac{RT}{b} \ln(aC_e) \tag{10}$$

A linear form of the Temkin isotherm can be expressed as:

$$q_e = \frac{RT}{b} \ln A + \frac{RT}{b} \ln C_e \tag{11}$$

$$q_e = B \ln A + B \ln C_e \tag{12}$$

where R is gas constant (8.314 J mol^{-1} K^{-1}), T is temperature (K), A is the equilibrium binding constant (L/g) corresponding to the maximum binding energy, and constant $B = RT/b$ is related to the heat of adsorption. A plot of q_e versus $\ln C_e$ (Fig. 5b) is used to calculate the Temkin isotherm constants A and B. Fig. 5a and b illustrates that the adsorption of Sr^{2+} ions fitted well the Freundlich and Temkin isotherm models, thereby implying that the adsorption may occur as a heterogeneous surface adsorption. The Freundlich and Temkin isotherm model constants are given in Table 2.

3.7. Adsorption thermodynamics

Adsorption experiments were also performed to obtain the thermodynamic parameters. The adsorption capacity decreases with the increase of temperature thus suggesting the exothermic nature of the adsorption process and the weakening of bonds between Sr^{2+} and active sites of adsorbents at high temperatures (Table 1). A plot of $\log(q_e/C_e)$ versus $1/T$ is displayed in Fig. 5c. The thermodynamic parameters ΔG, ΔH and ΔS were calculated using vant-Hoff equation (Eq. (13)), and are tabulated in Table 3. The negative ΔG values ascertain the spontaneity of the adsorption process.

$$\log\left(\frac{q_e}{C_e}\right) = -\frac{\Delta H}{2.303RT} + \frac{\Delta S}{2.303R} \tag{13}$$

As the temperature increases, the ΔG values become less negative, indicating that the adsorption process is less favorable at the higher temperatures. The negative ΔH of -15.7 kJ mol^{-1} indicates the exothermic nature of the adsorption process; similar exothermic behavior ($\Delta H = -5.9$ and -5.2 kJ mol^{-1}) has been noted in two different reports describing the adsorption of Sr^{2+} on polyacrylonitrile/zeolite composite adsorbent [6] and Dowex 50W-X Resins [16]. The negative value of ΔS (-39.5 J mol^{-1} K^{-1}) is quite unexpected, however it suggests the decrease in randomness at the solid/solution interface during the adsorption process as a result of replacement of Na$^+$ with Sr^{2+}.

3.8. Desorption experiment

Desorption experiment was conducted to study the sorbent regeneration options. Sr^{2+} ions in the loaded resin were desorbed by stirring in a 0.1 M HNO$_3$ medium. The results indicated that the percentage efficiency of the desorption process to be 88%.

3.9. SEM and EDX images for CPZ **4** and CPZE **5** unloaded and loaded with Sr^{2+} ions

Unloaded CPZ **4** and CPZA **5** as well as loaded resin **5** were investigated by scanning electron microscopy (SEM). Unloaded resin (60 mg) were immersed in Sr(NO$_3$)$_2$ solution (500 ppm in Sr^{2+}, 20 mL) for 24 h at a pH of 3, filtered, and dried under vacuum until constant weight was achieved. Loaded and unloaded polymers were then sputter-coated for 2 min with a thin film of gold.

SEM and EDX images (Fig. 6) show that the morphology has been altered by the adsorption of Sr^{2+} ions (cracked morphology to smooth); the EDX analysis (Fig. 6a and b) shows that composition of unloaded CPZ **4** and CPZA **5** was similar to the proposed in scheme 1, while the former has more tight surface morphology as a result of H-bonding involving COOH, the later confirms the presence of Na$^+$ with an open morphology as a result of repulsion between the negative charges of the CO$_2^-$. Fig. 6c shows that the Sr^{2+} ions have displaced the sodium ions in CPZA **5** thus confirming the adsorption of the metal ions. The SEM and EDX confirmed that CPZA **5** could be used as an efficient adsorbent of Sr^{2+} in aqueous solutions at low concentrations.

4. Conclusion

A novel cross-linked polyzwitterion/anion (CPZA) was prepared using Butler's cyclopolymerization protocol. The CPZA provided an opportunity to test the efficacy of a zwitterionic/anionic group in the removal of a model metal ion in low concentrations. The resin was found to have a very good adsorption capacity for Sr^{2+} ions at low concentrations. The relatively strong rapid initial adsorption of 83% Sr^{2+} ions was followed by slower adsorption of the remaining 17% which was described by intraparticle diffusion model. The adsorption followed pseudo-second-order kinetic model and Temkin as well as Freundlich isotherm models. The negative ΔGs and ΔH ensured the spontaneity and the exothermic nature of the adsorption process. The excellent adsorption and desorption efficiencies implied the efficacy of the resin in removing as well as recovering the metal ions from aqueous solution. Given that the efficiencies of many investigated materials towards Sr^{2+} were low at low pH, the current CPZA seems to be promising for the removal of Sr^{2+} from acidic media.

References

[1] D. Chakraborty, S. Maji, A. Bandyopadhyay, S. Basu, Bioresour. Technol. 98 (2007) 2949–2952.
[2] S. Chegrouche, A. Mellah, M. Barkat, Desalination 235 (2009) 306–318.
[3] C.W. Fetter, Contaminant Hydrogeology, second ed., Prentice Hall, Upper Saddle River, NJ, USA, 1999.
[4] A.Y. Zhang, Y.Z. Wei, M. Kumagai, React. Funct. Polym. 61 (2004) 191–202.
[5] R. Chang, Chemistry, eighth ed., McGraw-Hill, Boston, 2005. p328.
[6] S. Yusan, S. Erenturk, J. Nucl. Sci. Technol. 1 (2011) 6–12.
[7] S.A. Khan, Waste Manage. 15 (1995) 641–650.
[8] I. Smičiklas, S. Dimović, I. Plećaš, Appl. Clay Sci. 35 (2007) 139–144.
[9] T. Missana, M. Garcia-Gutierrez, Phys. Chem. Earth 32 (2007) 559–567.

[10] A.Y. Zhang, W.H. Wang, Z.F. Chai, M. Kumagai, J. Sep. Sci. 31 (2008) 3148–3155.
[11] A. Zhang, Y.Z. Wei, M. Kumagai, T. Koyama, J. Radioanal. Nucl. Chem. 262 (2004) 739–744.
[12] E.H. Rifi, F. Rastegar, J.P. Brunette, Talanta 42 (1995) 811–816.
[13] C. Ozeroglu, G. Keceli, J. Radioanal. Nucl. Chem. 268 (2006) 211–219.
[14] M. Wang, L. Xua, J. Peng, M. Zhai, J. Li, G. Wei, J. Hazard. Mater. 171 (2009) 820–826.
[15] S. Komarneni, T. Kodama, W.J. Paulus, J. Mater. Res. 15 (2000) 1254–1256.
[16] M. Hafizi, H. Abolghasemi, M. Moradi, S.A. Milani, J. Chin. Chem. Eng. 19 (2011) 267–272.
[17] M. Nyman, A. Tripathi, J.B. Parise, R.S. Maxwell, T.M. Nenoff, J. Am. Chem. Soc. 124 (2002) 1704–1713.
[18] E.A. Behrens, P. Sylvester, A. Clearfield, Environ. Sci. Technol. 32 (1998) 101–107.
[19] S. Komarneni, T. Kodama, W.J. Paulus, C. Carson, J. Mater. Res. 15 (2000) 1254–1256.
[20] R. Chiarizia, D.R. McAlister, A.W. Herlinger, Solvent Extr. Ion Exc. 21 (2003) 171–197.
[21] R.S. Herbst, J.D. Law, T.A. Todd, V.N. Romanovskiy, et al., Solvent Extr. Ion Exc. 20 (2002) 429–445.
[22] H. Luo, S. Dai, P.V. Bonnesen, Anal. Chem. 76 (2004) 2773–2779.
[23] G. Garg, G.S. Chauhan, J. Ahn, Polym. Adv. Technol. 22 (2011) 1794–1801.
[24] A.V. Dobrynin, R.H. Colby, M. Rubinstein, J. Polym. Sci. Part B: Polym. Phys. 42 (2004) 3513–3538.
[25] S.E. Kudaibergenov, Polyampholytes: Synthesis, Characterization and Application, Kluwer Academic/Plenum Publishers, New York, 2002.
[26] S.E. Kudaibergenov, W. Jaeger, A. Laschewsky, Adv. Polym. Sci. 201 (2006) 157–224.
[27] A.B. Lowe, N.C. Billingham, S.P. Armes, Macromolecules 32 (1999) 2141–2148.
[28] Y. Umar, B.F. Abu-Sharkh, S.A. Ali, Polymer 46 (2005) 10709–10717.
[29] J. Liu, Y. Ma, T. Xu, G. Shao, J. Hazard. Mater. 178 (2010) 1021–1029.
[30] J. Liu, Y. Ma, Y. Zhang, G. Shao, J. Hazard. Mater. 173 (2010) 438–444.
[31] W. Liang, C. Wu, C. Hsu, P. Kuo, J. Polym. Sci. A: Polym. Chem. 44 (2006) 3444–3453.
[32] H.A. Al-Muallem, M.I.M. Wazeer, S.A. Ali, Polymer 43 (2002) 1041–1050.
[33] S.A. Haladu, S.A. Ali, Eur. Polym. J. doi: 10.1016/j.eurpolymj.2013.02.007.
[34] S.A. Ali, S.Z. Ahmed, E.Z. Hamad, J. Appl. Polym. Sci. 61 (1996) 1077–1085.
[35] G.B. Butler, J. Polym. Sci. A: Polym. Chem. 34 (1996) 913–923.
[36] G.B. Butler, J. Polym. Sci. Part A: Polym. Chem. 38 (2000) 3451–3461.
[37] G.B. Butler, Cyclopolymerization and Cyclocopolymerization, Marcel Dekker, New York, 1992.
[38] O.C.S. Al Hamouz, S.A. Ali, Sep. Purif. Technol. 98 (2012) 94–101.
[39] H.S. Martinez-tapia, A. Cabeza, H. Bruque, P. Pertierra, S. Garcmh, M.A.G. Aranda, J. Solid State Chem. 151 (2000) 122–129.
[40] S.A. Ali, H.A. Al-Muallem, M.A.J. Mazumdar, Polymer 44 (2003) 1671–1679.
[41] H.A. Al-Muallem, M.I.M. Wazeer, S.A. Ali, Polymer 43 (2002) 4285–4295.
[42] S.K. Sahni, R.V. Bennekom, J. Reedijk, Polyhedron 4 (1985) 1643–1658.
[43] D. Kolodynska, Z. Hubicki, S. Pasieczna-Patkowska, Acta. Phys. Pol. A 116 (2009) 340–343.
[44] Q. Li, H. Liu, T. Liu, M. Guo, B. Qing, X. Ye, Z. Wu, Chem. Eng. J. 157 (2010) 401–407.
[45] G. Garga, G.S. Chauhana, J. Ahn, Polym. Adv. Technol. 22 (2011) 1794–1801.
[46] T.D. Duong, K.L. Nguyen, M. Hoang, J. Colloid Interface Sci. 301 (2006) 446–451.
[47] S. Lagergren, K. Sven, Vetenskapsakad. Handl. 24 (1898) 1–39.
[48] A. Ramesh, H. Hasegawa, T. Maki, K. Ueda, Sep. Purif. Technol. 56 (2007) 90–100.
[49] Y.S. Ho, G. McKay, Process Biochem. 34 (1999) 451–465.
[50] M. Minceva, L. Markovska, V. Meshko, Chem. Eng. 26 (2007) 125–134.
[51] Y. Lin, H. Chen, K. Lin, B. Chen, C. Chiou, J. Environ. Sci. 23 (2011) 44–50.
[52] W.J. Weber, J.C. Morris, Eng. Div. Am. Soc. Civ. Eng. 89 (1963) 31–60.
[53] F.C. Wua, R.L. Tseng, R.S. Juang, Chem. Eng. J. 153 (2009) 1–8.
[54] J. Liu, J. Si, Q. Zhang, J. Zheng, C. Han, G. Shao, Ind. Eng. Chem. Res. 50 (2011) 8645–8657.
[55] A. Ozcan, A.S. Ozcan, O. Gok, Adsorption kinetics and isotherms of anionic dye of reactive blue 19 from aqueous solutions onto DTMA-sepiolite, in: A.A. Lewinsky (Ed.), Hazardous Materials and Wastewater-Treatment, Removal and Analysis, Nova Science Publishers, New York, 2007.
[56] K. Vijayaraghavan, T.V.N. Padmesh, K. Palanivelu, M. Velan, J. Hazard. Mater. B133 (2006) 304–308.
[57] S. Kundu, A.K. Gupta, Chem. Eng. J. 122 (2006) 93–106.
[58] F. Haghseresht, G. Lu, Energy Fuel 12 (1998) 1100–1107.
[59] B. Alyüz, S. Veli, J. Hazard. Mater. 167 (2009) 482–488.
[60] J. Liu, L. Song, G. Shao, J. Chem. Eng. Data 56 (2011) 2119–2127.